Journal of Applied Microbiology, 2023, 134, 1–12
https://doi.org/10.1093/jambio/lxad158
Advance access publication date: 21 July 2023
Research Article

JOURNAL OF APPLIED MICROBIOLOGY
OXFORD UNIVERSITY PRESS

Discovery and structural assignment of (S)-sydosine from amphipod-derived *Aspergillus sydowii* MBC15-11F through HRMS, advanced Mosher, and molecular modelling analyses

Mallique Qader [1,2,13], Larry L. Mweetwa[3], Teppo Rämä [4], Bathini Thissera[1], Bruce F. Milne[5,6], Usama R. Abdelmohsen [7,8], Raha Orfali[9], Ahmed Tawfike[10], Manal Esheli[1,11], Emmanuel T. Oluwabusola[3,12], Lalith Jaysainghe[2], Marcel Jaspars[3], Mostafa E. Rateb[1,*]

[1]School of Computing, Engineering and Physical Sciences, University of the West of Scotland, Paisley PA1 2BE, Scotland, UK
[2]National Institute of Fundamental Studies, Hantana Road, Kandy 20000, Sri Lanka
[3]Marine Biodiscovery Centre, Department of Chemistry, University of Aberdeen, Old Aberdeen AB24 3UE, UK
[4]The Norwegian College of Fishery Science, UiT Arctic University of Norway, Tromsø 9019, Norway
[5]Department of Physics, University of Coimbra, Rua Larga, 3004-516 Coimbra, Portugal
[6]Department of Chemistry, University of Aberdeen, Old Aberdeen AB24 3UE, Scotland, UK
[7]Department of Pharmacognosy, Faculty of Pharmacy, Minia University, Minia 61519, Egypt
[8]Department of Pharmacognosy, Faculty of Pharmacy, Deraya University, New Minia 61111, Egypt
[9]Department of Pharmacognosy, College of Pharmacy, King Saud University, Riyadh 11451, Saudi Arabia
[10]Department of Pharmacognosy, Faculty of Pharmacy, Helwan University, 11795 Cairo, Egypt
[11]Food Science & Technology Department, Faculty of Agriculture, University of Tripoli, Tripoli 13538, Libya
[12]DDT College of Medicine, Broadhurst Mall, P.O. Box 70587, Gaborone, Botswana

*Corresponding author. School of Computing, Engineering and Physical Sciences, University of the West of Scotland, Paisley PA1 2BE, Scotland, UK. E-mail: Mostafa.Rateb@uws.ac.uk
[13]Present address- Institute for Tuberculosis Research, Department of Pharmaceutical Sciences, University of Illinois Chicago, 833 South Wood St, Chicago, 60612 Illinois, USA

Abstract

Aims: This study aims to prioritize fungal strains recovered from under-explored habitats that produce new metabolites. HRMS dereplication is used to avoid structure redundancy, and molecular modelling is used to assign absolute configuration.

Methods and results: MBC15-11F was isolated from an amphipod and identified using ITS, 28S, and β-tubulin phylogeny as *Aspergillus sydowii*. Chemical profiling using taxonomic-based dereplication identified structurally diverse metabolites, including unreported ones. Large-scale fermentation led to the discovery of a new *N*-acyl adenosine derivative: (S)-sydosine (**1**) which was elucidated by NMR and HRESIMS analyses. Two known compounds were also identified as predicted by the initial dereplication process. Due to scarcity of **1**, molecular modelling was used to assign its absolute configuration without hydrolysis, and is supported by advanced Mosher derivatization. When the isolated compounds were assessed against a panel of bacterial pathogens, only phenamide (**3**) showed anti-*Staphylococcus aureus* activity.

Conclusion: Fermentation of *A. sydowii* yielded a new (S)-sydosine and known metabolites as predicted by HRESIMS-aided dereplication. Molecular modelling prediction of the absolute configuration of **1** agreed with advanced Mosher analysis.

Significance and impact of study

HRESIMS-based dereplication is a fast and reliable technique for the prioritization of microbial strains recovered from under-explored habitats. Additionally, molecular modelling was used for the determination of the absolute configuration of a sugar-containing metabolite.

Keywords: *Aspergillus sydowii*, deap-sea, (S)-sydosine, HRMS, dereplication, molecular modelling

Introduction

Fungi are eukaryotic organisms widely distributed in every possible micro and macro-environment of the planet (Zain ul Arifeen et al. 2019). Fungi are the most prolific producers of new chemical compounds reported from the marine environment. In 2019, 47% of the 1490 new natural products reported from marine environments were sourced from fungi, and by the end of 2019, ~5300 new natural products had been isolated from marine fungi (Carroll et al. 2021). The diversity of marine metabolites may result of stresses on organisms in marine habitats, including high salinity, low temperature, high pressure, low light, or a combination of conditions (Sayed et al. 2020). This is particularly true for deep-sea fungi that reside at depths of thousands of metres below the surface (Debbab et al. 2010). A high diversity of species survives under such conditions and produces structurally novel natural products, with almost a quarter of marine natural products having no terrestrial equiv-

Received: May 16, 2023. **Revised:** July 12, 2023. **Accepted:** July 20, 2023

alent (Bhakuni and Rawat 2005, Voser et al. 2022). It is postulated that the fungal genome has evolved to sustain these organisms in harsh environments (Zain ul Arifeen et al. 2019).

The genus *Aspergillus* is known as a major producer of marine fungal secondary metabolites, accounting for ∼19% of all discovered marine fungal metabolites during the period 1992–2019 (Orfali et al. 2021). Many new bioactive alkaloids, peptides (cyclic and open chain), polyketides, terpenoids, and xanthones have been identified from different marine Aspergilli, which possess diverse biological effects, including antimicrobial, anticancer, anti-inflammatory, antidiabetic, and neuroprotective (Orfali et al. 2021). *Aspergillus sydowii* produces diverse metabolites; for example, over 30 metabolites structurally related to sydonic acid and sydowinin have been reported in the literature (Hayashi et al. 2016). Many *A. sydowii* strains have been recovered from marine habitats. They are known to be the causative agent of the aspergillosis disease of the Gorgonian corals and have had a significant impact on their population decline in the Caribbean (Ein-Gil et al. 2009). However, *A. sydowii* is not restricted in its occurrence to tropical marine habitats but is a widespread ubiquitous fungus and opportunistic pathogen that has also been isolated from colder waters (Li et al. 2018, Niu et al. 2020), such as deep-sea sediments or glaciers, as well as from clinical patients and natural non-marine habitats (Rypien et al. 2008).

Dereplication is a technique used to quickly identify already known secondary metabolites from an extract (Tawfike et al. 2013, Abdelmohsen et al. 2014). This process is hampered by the fact that metabolites exist in the crude extract at various concentrations and have different chemical and physical properties. Molecular weight-based dereplication plays a key role in the metabolite identification process. Up to date, advanced HRMS instruments can unveil the chemical profile in terms of their accurate mass, HRMS/MS data, and UV data (Kildgaard et al. 2014). The advantage of the LC–HRMS dereplication is the quick discovery of new secondary metabolites without wasting time and resources. Further analysis of accurate mass in the databases such as Dictionary of Natural Products, AntiBase, AntiMarin, MarinLit, amongst others may achieve the main objective of the dereplication (Kildgaard et al. 2014).

In a continuation of our studies on searching for bioactive microbial metabolites from marine-derived fungi, the fungal strain *Aspergillus sydowii* MBC15-11F, together with other fungi, was recovered from the lumen sample of the cosmopolitan deep-sea amphipod *Eurythenes gryllus* that was collected from the North Atlantic Ocean. The chemical profiling of the crude extracts of these fungi was performed using LC–HRMS-based dereplication analysis. This approach allowed us to prioritize the MBC15-11F extract, which had a new hit that was not dereplicated using available natural product databases. Hence, large-scale fermentation, fractionation, and purification of MBC15-11F extract using flash column chromatography and semi-preparative RP–HPLC yielded a new *N*-acyl adenosine alkaloid: (S)-sydosine (**1**), and two known metabolites brefeldin A (**2**), and phenamide (**3**). Herein, we report the strain isolation, molecular identification, chemical profiling using LC–HRMS dereplication analysis, large-scale cultivation, isolation, and structural characterization of the new compound, and the antimicrobial effect of the isolated metabolites. Additionally, we report the use of advanced Mosher ester and molecular modelling to assign the absolute configuration of (S)-sydosine without hydrolysis.

Materials and methods

Isolation of the fungal strain MBC15-11F

The strain MBC15-11F was isolated from the lumen of the cosmopolitan deep-sea amphipod *Eurythenes gryllus* collected by Dr Alan Jamieson, University of Aberdeen, from the North Atlantic Ocean during dive 3 on Scotia Vessel's cruise number 0915S in July 2015 using a baited lander sampling gear. The sample was collected at 57.954542 N 15.55947 W and preserved at −20°C in a 50-mL falcon tube for later processing. The amphipod sample was processed by mechanical homogenization of 1 g of its lumen tissue using a sterile mortar and pestle. A portion of this mixture (1 mL) was transferred to 9 mL of sterile seawater. To further reduce the bacterial colony numbers, successive serial dilutions were conducted in ratios of 10^{-1} to 10^{-5}. Approximately 100 μL was inoculated onto malt extract agar plates and incubated at 15°C for 3–4 weeks. The agar plates were monitored regularly. Plates that showed growth were distinguished and the dominant types of fungal colonies were re-isolated on corresponding media, where the growth pattern was excellent. The plates were incubated at 25°C for 48–72 h. The pure colonies were isolated and selected based on physical characteristics, colour, colony size, and unique morphology. Pure cultures were kept frozen for further studies at −80°C in malt extract liquid media supplemented with 50% glycerol. A stock culture was preserved at the University of the West of Scotland, UK, under the code of MR-MBC15-11F.

Identification of the deep-sea fungus MBC15-11F

MBC15-11F was sub-cultured on a 4-g malt extract broth (Jensen & Co, Nittedal, Norway) and 15 g of agar (Sigma, St. Louis, MO, USA) in 1 L of artificial seawater prepared by dissolving 40 g Sigma Sea salts in Milli-Q H_2O (Millipore, Bedford, MA, USA). DNA was extracted from a pure isolate using a modified cetyltrimethylammonium bromide (CTAB) extraction procedure (Murray and Thompson 1980) following Rämä et al. (Rämä et al. 2017) with the exception that cell lysis was done using beads bashing by running the samples in a FastPrep 24 homogenizer (MP Biomedicals, USA) for 20 s at the speed of 4 m/s. PCR amplification of the marker genes was performed on an Eppendorf Mastercycler EP Gradient S (Eppendorf AG, Hamburg, Germany) using the primer pairs and cyclic PCR programs specified in Table S1. One microlitre of forward and reverse primers were used in 0.5 mM concentration, 12.5 µL of DreamTaq Green PCR Master Mix 2X (Thermo Fisher Scientific), 10.5 µL of Milli-Q H_2O, and 1 µL DNA template in a reaction volume of 25 μL. The PCR products were cleaned using an A'SAP PCR clean-up kit (ArcticZymes, Tromsø, Norway) according to the manufacturer's instructions. The purified PCR products were prepared for Sanger sequencing using BigDye3.1 and a PCR program consisting of initial denaturation of 1 min at 95°C, 40 cycles at 95°C for 5 s, 47°C for 30 s, and 60°C for 4 min. The sequencing was performed using PCR primers as sequencing primers and an Applied Biosystems 3130xl Genetic Analyzer (Foster City, CA, USA) at the University Hospital of North Norway. Returned chromatograms were imported into Geneious Prime

Table 1. Overview of the fungal isolates and sequences used in the phylogenetic analyses.

Isolate	ITS	28S	tub2
A. versicolor ATCC 9577 TYPE	NR_131277.1	NG_055743.1	KU897001.1
A. versicolor CBS 137.55	MH857417.1	MH868955.1	-
A. sydowii UTHSC 06–2780	LN898721.1	-	LN898875.1
A. sydowii UTHSC 06–2186	LN898720.1	-	LN898874.1
A. sydowii UTHSC 10–1222	LN898727.1	-	LN898881.1
A. sydowii CBS 593.65 TYPE	NR_131259.1	-	EF428373.1
A. sydowii UTHSC 07–1018	LN898723.1	-	LN898877.1
A. raperi NRRL 2641 TYPE	NR_135351.1	NG_064014.1	EF652278.1
A. asper NRRL 35910 TYPE	NR_151788.1	NG_070046.1	KT698838.1
MBC15-11F	**OK664991**	**OK664992**	**OK66836**
P. antarcticum CBS 100 492	MH862703.1	NG_064177.1	MN969371.1

GenBank (Benson et al. 2014) accession numbers are given for each sequence and the study isolate is in bold font.

2021.2.2 (Biomatters Ltd, Auckland, New Zealand), assembled into consensus sequences, and manually inspected.

Preliminary BLAST analyses using the consensus sequences from nuclear rRNA and protein-coding genes suggested that the isolate MBC15-11F was most closely related to *Aspergillus sydowii*, followed by another related species, *A. versicolor*. Internal transcribed spacers region (ITS), large subunit ribosomal RNA gene (28S), and β-tubulin (tub2) sequences derived from 10 *Aspergillus* and 1 *Penicillium* isolates were downloaded and used in a phylogenetic analysis to verify the identity of MBC-11F (Table 1). Taxonomic identification of the isolate MBC15-11F was based on Bayesian inference and maximum likelihood. The sequences generated for this study are deposited at GenBank (Benson et al. 2005) with the accession numbers specified in Table 1.

All analysed sequences were aligned using MAFFT v.7.450 (Katoh et al. 2002, Katoh and Standley 2013) with automatic alignment algorithm selection based on the data, scoring matrix 1000PAM/k = 2, gap open penalty of 2.53, and offset value of 0.123 in Geneious Prime. The resulting alignment was manually improved and cut at the 3′ and 5′ ends, resulting in the final alignment that contained 11 taxa and was 1451 bp long. The evolutionary model selection for the phylogenetic analysis was done in Smart Model Selection in PhyML (Lefort et al. 2017) using five partitions: ITS1, 5.8S, ITS2, 28S, and TUB2. A general time reversible (GTR) model was suggested for 5.8S, GTS with γ-distributed rate variation across sites for ITS2 and 28S, and GTR with proportion of invariable sites for ITS1 and tub2 based on Akaike Information Criteria. The analysis was set up using the partitions, suggested evolutionary models, and default priors. The parameters were unlinked across partitions and the Markov chain Monte Carlo (MCMC) analysis was run using two parallel runs with four chains and 0.2 temperature of the heated chains in MrBayes 3.2.6 (Huelsenbeck and Ronquist 2001). *Penicillium antarcticum* was used as an outgroup. The MCMC runs reached stationary with an average frequency of split frequency being <0.01 and based on visual inspection of the MCMC trace. One-fourth of the samples were discarded as burnin and the resulting 2001 trees from each run were used to create the consensus phylogram. The same alignment with the same partitions and evolutionary models was used to run a maximum likelihood analysis using 10 000 bootstrap replicates in RAxML (Stamatakis 2006, 2014). The topology of the RAxML tree (not shown) was identical to the Bayesian tree and the bootstrap support values for the nodes are given with the Bayesian tree in Fig. 1.

General procedure for chemical profiling

The microbial extract was prepared for mass spectrometry analysis according to Abdelmohsen et al. (Abdelmohsen et al. 2014). The acquired data were processed using MZmine 2.20 by applying standard parameters (Lotfy et al. 2021). Finally, the peaks were dereplicated against the Dictionary of Natural Product database. A detailed chemical profiling process is presented in the section "Materials and methods" of the Supplementary Material.

Small- and large-scale fermentation and extraction

The pure fungal isolate was cultivated in marine ISP2 agar (sea salt incorporated) containing 0.1% nalidixic acid (Sigma–Aldrich, UK) as a broad-spectrum antibacterial agent and incubated for 5−7 days at room temperature. Once the inoculated fungus grew equally throughout the agar plate, two equal size agar pieces with the fungus were aseptically introduced into 3 L × 12 conical flasks containing 1 L of marine ISP2 broth media. They were subjected to static fermentation for 30 days without agitation. After the fermentation period, the mycelial mat was removed and extracted with methanol (MeOH; 3 × 500 mL). Approximately 5 g/L of Diaion HP20 was added to the broth and centrifuged (180 rpm) for 6 hr. Then, Diaion HP20 was filtered and extracted with MeOH (3 × 500 mL). Both MeOH extracts were combined and evaporated under a vacuum to get the crude extract and subsequently fractionated with *n*-hexane, dichloromethane (DCM), and ethyl acetate (EtOAc). LC–HRMS analysis indicated the presence of the unknown hit and similar metabolite pattern in both DCM and EtOAc fractions. Hence, they were combined before further purification took place.

Isolation of fungal metabolites

Combined extracts (1.8 g) were purified using flash chromatography using silica gel 0.03−0.20 packed in a glass column (diameter 3.5 cm) and eluted with different solvent ratios of *n*-hexane:DCM:MeOH—1:0:0 to 0:1:0 and 0:1:0 to 0:0:1 in different polarities. Each collection was examined using TLC (10% MeOH:DCM) and pooled accordingly resulting five subfractions. Each sub-fraction was analysed using RP−HPLC (Phenomenex RP−C18 analytical column (Luna 5 μm, 250 × 4.60 mm, L × i.d.) using 1.5 mL/min flow rate and 10%−100% of acetonitrile (MeCN) in H_2O gradient over 30 min and 100% MeCN for 5 min. HPLC chromatogram showed a similar pattern in the third and fourth subfractions. Therefore, both were combined and further purified using semi-preparative Sunfire RP−C18 column (Sunfire 5 μm, 250 × 10 mm, L × i.d.) using a gradient of MeCN in H_2O as eluent (MeCN 10%−100% for 50 min and 100% MeCN for 10 min) at a flow rate of 1.5 mL/min, to afford new adenosine derivative: sydosine (**1**, 1.1 mg) and two known brefeldin A (**2**, 7 mg), and phenamide (**3**, 2.4 mg) metabolites.

(+)(S)-Sydosine (**1**): white crystalline solid; +12.65 (c 0.01, MeOH); UV (MeOH) λmax (log ε): 205 (3.90), 214 (3.55), 224 (2.90); ^{1}H NMR (600 MHz, DMSO−d_6) and ^{13}C NMR (150 MHz, DMSO−d_6): HR−ESIMS: $[M + H]^+$ at m/z 416.1568 $C_{19}H_{21}N_5O_6$ (calcd. 416.1564).

Brefeldin A (**2**): colourless crystals; +91.05 (c 0.1, MeOH—compared to + 92.2 [51]); UV (MeOH) λmax (log ε): 205 (4.20), 214 (3.65), 224 (3.10); ^{1}H NMR (600 MHz, DMSO−d_6): δ 0.75−1.75 (2H, m), 1.19 (3H, d, J = 6.84 Hz), 1.29−1.97 (2H, m), 1.47−1.71 (2H, m), 1.65−1.82 (2H, m), 1.70 (1H, m), 1.70−1.92 (2H, m), 2.31 (1H, m), 3.92 (1H, m), 4.04 (1H, m), 4.70 (1H, m), 5.19 (1H, m), 5.66 (1H, m), 5.71 (1H, d, J = 15.5 Hz), 7.34 (1H, d, J = 15.4 Hz); ^{13}C NMR (150 MHz, DMSO−d_6): δ 20.7, 26.5, 31.5, 33.4, 40.9, 43.1, 43.3, 51.3, 70.5, 70.9, 74.3, 116.3, 129.2, 137.1, 154.4, 165.7; HR−ESIMS: $[M + H]^+$ at m/z 281.1761 (Gorst-Allman et al. 1982, Glaser et al. 2000).

Phenamide (**3**): white amorphous solid, UV (MeOH) λmax (log ε): 205 (3.70), 254 (3.15); ^{1}H NMR (600 MHz, DMSO−d_6): δ 1.04 (3H, s), 1.21 (3H, s), 2.35−2.48 (2H, dd, J = 15.5 Hz), 2.81−3.17 (2H, m), 4.43 (1H, t, J = 4.7 Hz), 7.16−7.28 (5H, m); ^{13}C NMR (150 MHz, DMSO−d_6): δ 24.9, 25.5, 38.1, 43.5, 53.2, 56.5, 126.9, 128.8, 129.5, 139.2, 171.4, 178.1, HR−ESIMS: $[M + H]^+$ at m/z 265.1553 (Makkar et al. 1995).

Determination of absolute stereochemistry by Mosher ester reaction

The Mosher ester reaction between S and R was performed as described by Ohtani et al. (1991) and Su et al. (2002). The pure compound (0.5 mg each, 0.0012 mmol) was dissolved in 250 μL of deuterated pyridine and inserted into NMR tubes under N_2. Then, 0.5 mg (0.0021 mmol) of each (+R) and (−S) MTPA were measured separately and dissolved in 250 μL of deuterated pyridine under N_2 flow. Under a constant N_2 flow, prepared MTPA samples were immediately transferred to the NMR tubes. NMR tubes were thoroughly shaken to complete the reaction. The reaction was monitored by ^{1}H NMR and COSY after 5−6 hr to obtain the (+R) and (−S) MTPA esters. The chemical shift difference $[\Delta\delta^{S-R}$ (in ppm) $= \delta^{S} - \delta^{R}]$ was calculated from the ^{1}H NMR spectra of the two esters. The ^{1}H NMR spectrum of the pure compound in pyridine-d_5 was used as the reference sample to assign the signals.

Theoretical calculations

Conformational analysis of MTPA esters of 1

Structures for the (R)-MTPA and (S)-MTPA esters of **1** were built using the Avogadro software package (version 1.2; Hanwell et al. 2012). The lowest energy conformers of (R)-MTPA-1 and (S)-MTPA-1 were generated with the iterative metadynamics with genetic crossing (iMTD-GC) method implemented in the CREST software package (version 2.11.1) interfaced to the extended tight-binding semi-empirical electronic structure code xTB (version 6.4.0; Pracht et al. 2020, Grimme et al. 2021). The underlying electronic structure method used in the CREST calculations was the self-consistent charge tight-binding model GFN2-xTB, which includes the recent D4 density-dependent dispersion correction (Bannwarth et al. 2019, Bannwarth et al. 2021). The adaptive linearized Poisson–Boltzmann (ALPB) continuum solvent model was used for all xTB calculations (Caldeweyher et al. 2017, 2019, 2020). As the ALPB method in xTB was not parameterized for pyridine, THF was chosen as a substitute based on its dielectric constant, which is close to that of pyridine ($\varepsilon^{\text{pyridine}} = 12.4$, $\varepsilon^{\text{THF}} = 7.6$) and the fact that the two compounds are broadly similar, both being small heterocycles containing a single heteroatom and delocalized π-systems, meaning that in the continuum solvent approximation, their effect on calculations can also be expected to be very similar.

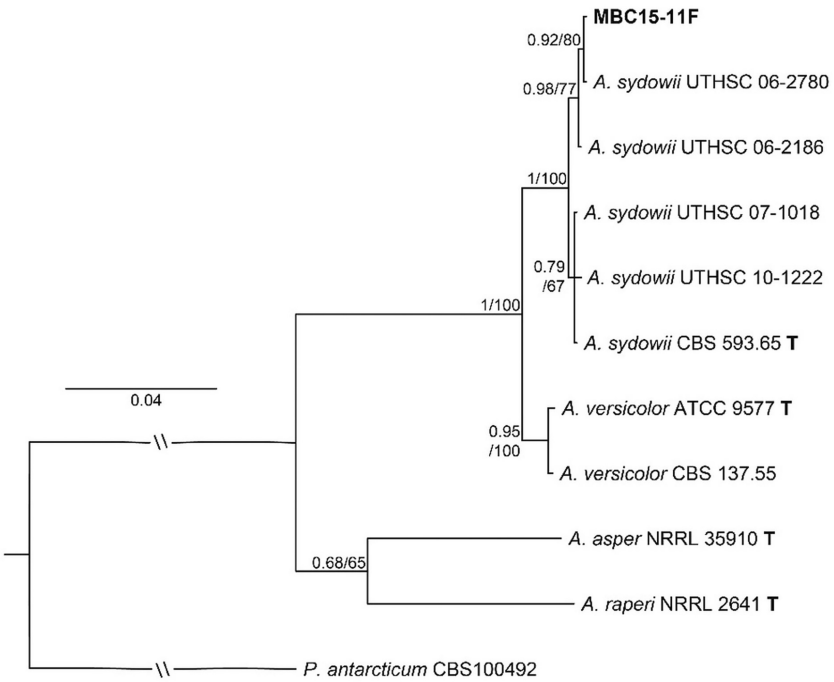

Figure 1. Phylogenetic tree of *Aspergillus sydowii* and *A. versicolor* isolates based on ITS, 28S, and tub2 sequences analysed using Bayesian inference. The studied isolate MBC15-11F is shown in bold. Isolate identifiers follow taxon names and node support is given as posterior probabilities/bootstrap support from the Maximum likelihood analysis. Sequences from type strains are marked with bold 'T'. *Penicillium antarcticum* was used as an outgroup for the other taxa. The scale bar shows estimated substitutions per site.

This choice was shown to lead to small changes in the energetics of a model of the aromatic core of **1** in subsequent DFT calculations (see below) and so is not expected to influence the results of the xTB calculations in any significant way.

Molecular dynamics of MTPA esters of 1

Ab-initio molecular dynamics (AIMD) simulations were performed on the lowest energy conformers obtained for (R)-MTPA-1 and (S)-MTPA-1 from the iMTD-GC CREST calculations. xTB was used in standalone mode for these calculations, which were performed with the GFN2-xTB method and ALPB THF solvation, as in the conformer generation step. Equilibration of 50 ps of each system at 298.15 K was performed to prepare the systems and avoid any heating effects on the data collection part of the simulations. The SHAKE algorithm was applied to all bonds and a timestep of 4 fs was used. The production phase involved 1 ns of simulation restarting directly from the equilibration runs and structures were sampled at 500 fs intervals for subsequent analysis. The 2000-structure AIMD trajectories were loaded into the UCSF Chimera package (Pettersen et al. 2004; version 1.16), and the distances between the MTPA chiral carbons and C–10 were extracted. The resulting time series were analysed using the Pandas (version 1.3.3) package in Python 3.9.5 (https://github.com/pandas-dev/pandas, accessed on 20 June 2022).

Density functional theory calculations of *cis/trans* amide preference in 1

A model of the core of **1** (Fig. S1) was built using Avogadro and energy was minimized at the DFT level using the Orca (Neese 2012, 2017) electronic structure package (version 5.0.0).

The r2SCAN meta-GGA DF approximation was used throughout along with the D4 dispersion correction (Furness 2020a, 2020b, Ehlert et al. 2021). Geometry optimization was performed with the triple-ζ Def2-TZVP basis set (Weigend and Ahlrichs 2005) using default integration grids and the resolution of the identity (RI) approximation for Coulomb interactions were employed with the Def/J auxiliary basis set (Weigend 2006). This was repeated for the *cis* and trans amide forms with THF and pyridine solvent effects modelled using the conductor-like polarizable continuum model (Tomasi et al. 2005; Mennucci 2012). The resulting structures were then submitted to final single-point calculations with the more accurate quadruple-ζ Def2-QZVP basis set (Ehlert et al. 2021) and the fine DefGrid3 integration grid to obtain accurate energies for the *cis* and trans isomers in both solvents.

Antimicrobial activity assay

Sample preparation and pathogenic bacterial strains

The isolated compounds were dissolved in 5% dimethyl sulfoxide (DMSO) to prepare stock solutions of 0.5 mg/mL. Pathogenic bacterial strains: *Staphylococcus aureus* ATCC25923, *Escherichia coli* NTCC12900, and *Pseudomonas aeruginosa* ATCC27853 were obtained from the Microbiology Department, University of the West of Scotland, UK.

Agar disk diffusion susceptibility test

The test was conducted by following the Kirby–Bauer disk diffusion susceptibility protocol (Hudzicki 2009) and EUCAST guidelines (https://www.eucast.org/ast_of_bacteria/disk_diffusion_methodology). Sterile disks (Sigma–Aldrich UK) were impregnated with 20 µL of a stock solution under sterile conditions. Each of the pathogenic inoculums was prepared in sterile saline solution at 0.5 McFarland standard. Each inoculum was inoculated (100 µL) into culture plates prepared with Muller–Hinton agar (Oxiod, UK). Sterile discs impregnated with compounds **1–3** and the reference standard antimicrobial rifampicin were placed on an agar surface and incubated at 35°C. Zones of inhibition were measured after 18–24 hr of incubation.

Calculation of MIC using microdilution method

The minimum inhibitory concentrations (MIC) of the compounds with susceptible inhibition zones in comparison to the standard reference were assessed by broth microdilution method in sterile 96-well plates (Thermo Scientific Ltd, Loughborough, UK) following the EUCAST guidelines (https://www.eucast.org/fileadmin/src/media/PDFs/EUCAST_files/MIC_testing/Reading_guide_BMD_v_ 3.0_2021.pdf) with slight modifications.

Results and discussion

Molecular identification of the fungus

Bayesian inference (BI) and maximum likelihood (ML) analyses show that the isolate MBC15-11F represents *Aspergillus sydowii* (Fig. 1). The analyses were run using a three-locus data matrix that contained sequences from eight closely related *A. sydowii* and *A. versicolor* isolates, including sequences from the type isolates of these species, and three other species represented by their type sequences. The BI and MI trees show the same topology and have the highest possible support value at the node, where the two species *A. sydowii* and *A. versicolor* branch off. Within the *A. sydowii* clade, there are two subclades: the type of isolate of the species being in the other subclade than MBC15-11F. The ITS, 28S, and tub2 sequences of the studied isolate of *A. sydowii* are very similar to the sequences of the isolate UTHSC 06–2780 isolated from human bronchus (Siqueira et al. 2016). It is not uncommon that some marine-derived isolates of fungi are genotypically highly similar or identical to non-marine-sourced isolates. This is especially true for *Aspergillus* species such as *A. flavus* (Ramírez-Camejo et al. 2012) and *A. sydowii* (Rypien et al. 2008).

Chemical profiling of the crude extract of MBC15-11F

The total MeOH crude extract of the strain was subjected to LC–HRESIMS analysis (Fig. S2). These metabolites were tentatively identified using natural product-specific databases. Our search was narrowed down to taxonomically related microbial metabolites to avoid misidentifications and misinterpretations. Additionally, identification of the metabolites using LC–HRMS analysis is based on matching two or more structural properties [e.g. accurate mass, isotope pattern, fragmentation pattern, retention time (R_t)]. This increased the accuracy of metabolite identification in the metabolomics experiment. Table 2 and Fig. 2 show the tentatively identified metabolites from MBC15-11F and their previously reported bioactivity.

Table 2. Fungal metabolites dereplicated from *Aspergillus sydowii* MBC15-11F.

Mode*	Accurate mass	R_t (min)	Molecular formula	Tentative identification	Reported bioactivity	Reported isolation	Ref.
P	180.0427	22.45	$C_9H_8O_4$	Dihydrocarolic acid (4)	CD45 tyrosine phosphatase inhibitor	*A. niger*	(Alvi et al. 2000)
P	192.0427	10.43	$C_{10}H_8O_4$	1,3,6,8-Naphthalenetetrol (5)	Melanin biosynthesis	*A. fumigatus*	(Tsai et al. 2001)
P	326.0427	29.47	$C_{17}H_{10}O_7$	Austocystin F (6)	Protein tyrosine phosphatases inhibitor	*A. ustus* marine *A. Puniceus*	(Steyn and Vleggaar 1974, Liang et al. 2021)
P	416.1568	19.78	$C_{19}H_{21}N_5O_6$	*No hits*	—	—	
P	340.1427	30.51	$C_{19}H_{20}N_2O_4$	Mactanamide (7)	Fungistatic against *Candida albicans*	marine *Aspergillus* sp.	(Lorenz et al. 1998)
P	352.1427	28.74	$C_{20}H_{20}N_2O_4$	N,N′-((1Z,3Z)-1,4-bis(4-methoxyphenyl)buta-1,3-diene-2,3-diyl)diformamide (8)	Cytotoxicity against lung, CNS, melanoma, ovarian, and renal carcinoma	*A. fumigatus* in coculture with *S. peucetius*	(Zuck et al. 2011)
P	265.1545	25.93	$C_{14}H_{20}N_2O_3$	Phenamide (3)	Fungicidal activity	—	Makkar et al. 1995)
P	606.3927	30.89	$C_{38}H_{54}O_6$	NF00659B2 (9)	Cytotoxic activities against human colorectal and ovarian carcinoma	*Aspergillus* sp. NF 00 659	Suzuki et al. 1997)
P	281.1749	20.86	$C_{16}H_{24}O_4$	Brefeldin A (2)	Induce apoptosis in leukemia, colon, and prostate cancer cell lines	mangrove-derived *Aspergillus* sp. 9Hu	(Huang et al. 2013)
P	705.2427	9.86	$C_{38}H_{35}N_5O_9$	Fumiquinazoline M (10)	Weak activity against murine lymphoma cancer cell line	sponge derived *Aspergillus* sp	(Zhou et al. 2013)
P	870.2927	15.52	$C_{33}H_{52}FeN_9O_{15}$	Asperchrome D (11)	Growth factor activity of *Arthrobacter flavescens* Jg-9.	*A. ochraceous*	(Jalal et al. 1984)

*P: Positive ionization mode.

Isolation and structure elucidation of secondary metabolites from MBC15-11F

A pure culture of *A. sydowii* MBC15-11F was fermented in modified ISP2 media (4 g/L of malt extract and glucose and 10 g/L of yeast extract, 1 L of distilled water with 15 g of sea salt incorporated) to obtain the crude MeOH extracts. Fractionation of the crude extract, followed by LC–HRMS analysis of these fractions indicated that both DCM and EtOAc fractions contain the unknown hit, thus they were combined for further analysis. Purification of combined DCM and EtOAc fractions over a series of chromatographic steps followed by semi-preparative RP–HPLC produced three fungal metabolites (**1–3**), including the new metabolite.

Compound **1** was obtained as a white crystalline solid. The NMR and the accurate mass analysis of **1** indicated a molecular formula of $C_{19}H_{21}N_5O_6$ with twelve double bond equivalents (DBE). HRESIMS analysis indicated a molecular ion peak of m/z 416.1562 $[M + H]^+$ (calcd. 416.1564 for $C_{19}H_{22}N_5O_6$). The NMR spectroscopic data (Table 3, Figs. S3–S9) showed that the molecule contained five sp^3-methines and seven sp^2-aromatic methines, two methylenes, and five quaternary carbons, including one carbonyl carbon at δ_C 169.9; accounting for a total of 19 carbons and 21 protons. Analysis of NMR data suggested the presence of aromatic sp^2-methines represented a monosubstituted benzene ring (δ_H 7.21/H–13/17, 7.27/H–14/16, 7.28/H–15), and two aromatic protons in a purine base (δ_H 8.13/H–3 and 8.35/H–6). Out of five, four sp^3-methines are accounted for the sugar moiety (δ_H 5.87/H–1′, 4.60/H–2′, 4.14/H–3′, 3.96/H–4′). The COSY spin system of H–1′ through H_2–5′ further supported the connections of the ribose sugar (Fig. 3). The HMBC correlation of the ribose anomeric proton (H–1′) to the purine ring at C–6 and C–4a confirmed the linkage of the ribose sugar to the N-containing heterocyclic purine base (Fig. 3).

The ^{1}H NMR spectra showed a cluster of peaks in the aromatic region at δ_H 7.21–7.28, which accounted for a monosubstituted benzene ring. The diastereotopic methylene at H_2–11 (δ_H 3.15 and 2.84) showed HMBC correlations to C–12 (δ_C 137.7) and C–13/17 (δ_C 126.3) of the benzene ring, and a COSY correlation to H–10 (δ_H 3.40). Additionally, both H–10 and H_2–11 showed strong HMBC correlations to the carbonyl carbon at δ_C 169.9 (C–9). These correlations confirmed the second substructure of the molecule to be 2-hydroxy-3-phenylpropanamide moiety.

The relative configuration of compound **1** was deduced by the NOESY experiment (Fig. 3, Fig. S10). The stereochemistry of the anomeric position of the ribose sugar moiety was assigned based on coupling constants and NOESY correlations. The NOESY correlation between the anomeric proton H–1′ and H–4′, and the adenine H–6 and H–2′ suggested the β anomer of the adenosine sugar moiety (Fig. 3), which is supported by the larger coupling constant of the anomeric proton (J = 6.5 Hz; Ciuffreda et al. 2007). In ribose sugars, the coupling constants of β-anomers between H–1′ and H–2′ is larger than that of α-anomers. The assignment of the β-adenosine moiety was confirmed by the ^{1}H and ^{13}C NMR chemical shift values of atom 1′ and other adenosine atoms together with coupling constants, which were in full agreement with literature data (Ciuffreda et al. 2007), the structure of compound **1** was deduced as a β-adenosine derivative to which the name sydosine is suggested as a new fungal secondary metabolite. To assign the absolute stereochemistry of

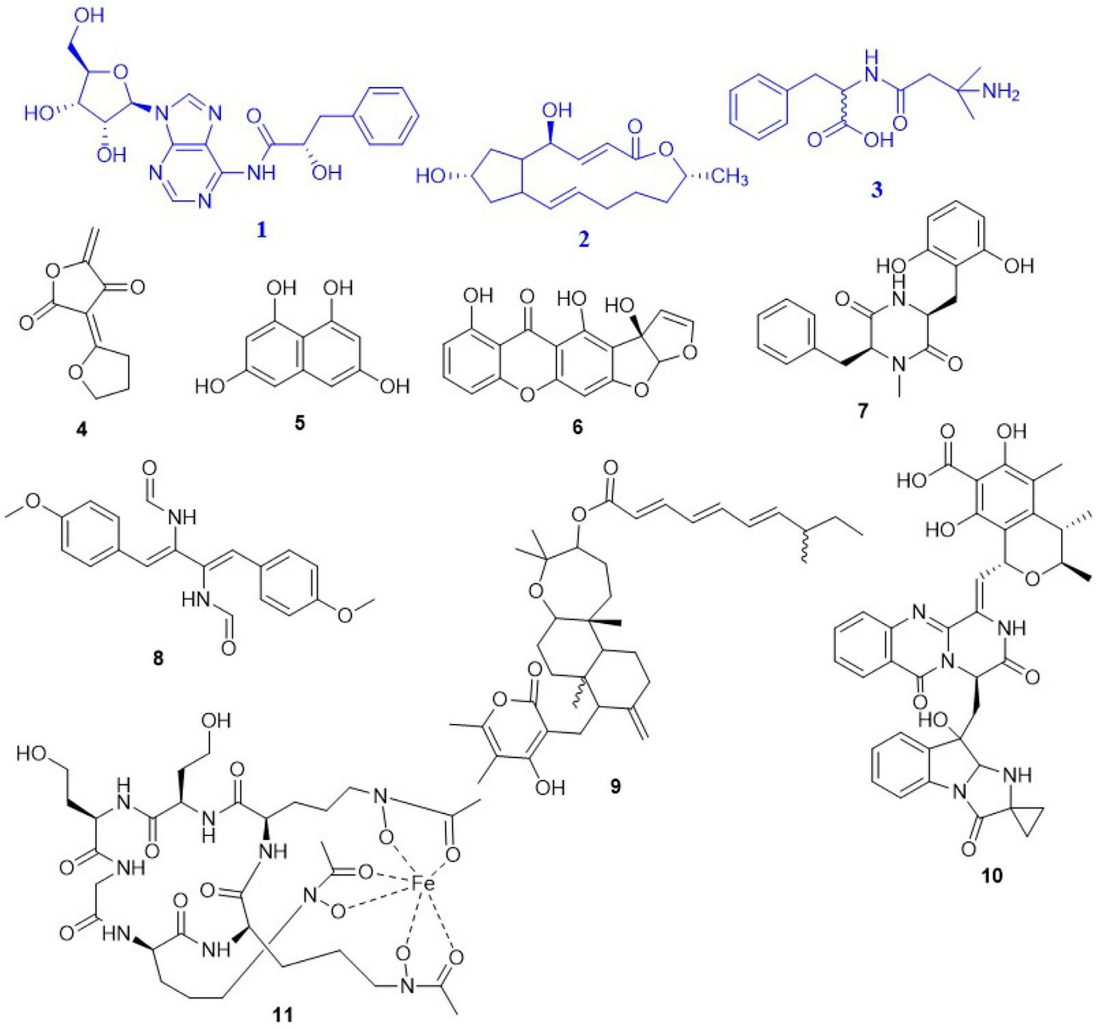

Figure 2. Tentatively identified and dereplicated compounds from HRMS data of the total MeOH crude extract of *A. sydowii* MBC15-11F using databases. Isolated metabolites from *Aspergillus sydowii* MBC15-11F are highlighted in blue.

Table 3. ^{1}H (600 MHz) and ^{13}C (150 MHz) NMR spectroscopic data for **1** (DMSO–d_6, 298 K).

No.	δ_H, mult. (*J* in Hz)	δ_C, type	COSY	HMBC
Adenosine moiety				
1	–	156.2, C	–	–
3	8.13 (*s*)	152.4, CH	–	C–7a, C–4a, C–1
4a	–	149.0, C	–	–
6	8.35 (*s*)	140.0, CH	–	C–1′
7a	–	119.4, C	–	–
8–NH	7.34 (*brs*)	–	–	–
1′	5.87 (*d*, 6.5)	87.9, CH	H–2′	C–6, C–2′, C–3′, C–4′, C–4a
2′	4.60 (*t*, 5.5)	73.5, CH	H–3′	C–1′, C–4′
3′	4.14 (*dd*, 3.1, 3.3)	70.7, CH	H–4′	C–1′, C–4′, C–5′
4′	3.96 (*dd*, 3.1, 4.4)	85.6, CH	H–5′	C–1′, C–5′
5′	3.68 (*dd*, 3.7, 12.1) 3.53 (*dd*, 3.7, 12.1)	61.7, CH_2	H–5′	C–3′
2-Hydroxy-3-phenylpropanamide moiety				
9	–	169.9, CO	–	–
10	3.40 (obscured)	55.6, CH	H–11	C–9, C–11
11	3.15 (*dd*, 4.8, 14.7) 2.84 (*dd*, 8.4, 14.4)	37.0, CH_2	H–11	C–9, C–10, C–13/17
12	–	137.7, C	–	–
13/17	7.21	126.3,	H–14,	C–15, C–12, C–11
14/16	7.29	128.4	H–13, H–15	C–12, C–15
15	7.26	129.3	H–14, H–16	C–14, C–16

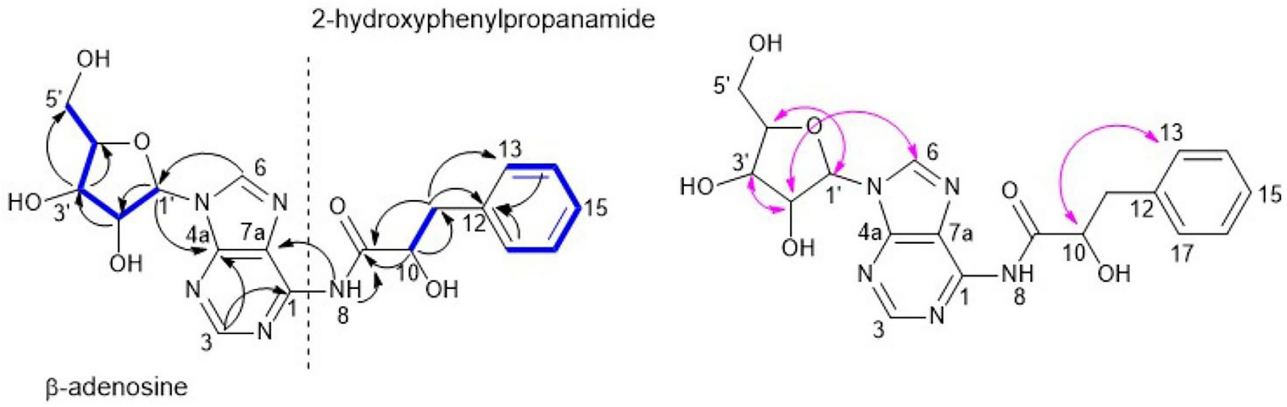

Figure 3. COSY (–), HMBC (arrows-black), and NOESY (arrows-pink) connectivity of compound **1**.

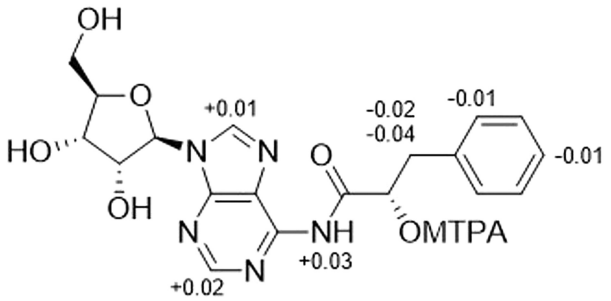

Figure 4. $\Delta\delta$ values [$\Delta\delta^{S-R}$ (in ppm) $= \delta^{S} - \delta^{R}$] obtained for the (S)- and (R)-MTPA esters of **1**.

1, the secondary alcoholic carbon (C–10) was modified as a Mosher ester, and NMR analysis of esterified **1** with (S) and (R)-MTPA was carried out (Figs.S11–S17). Significant chemical shift differences exhibited by the protons on the left (8-NH) and right (H_2–11, H–13, H–15) ligands confirmed the esterified 10-OH following MTPA treatment (Fig. 4) (Hoye et al. 2007, Seco et al. 2012). Considering the significant chemical shift differences associated with sugar protons (1′–5′; Table S2), the secondary OH groups at 2` and 3` were also deemed to be esterified together with the OH group at C–10. Therefore, it was important to assess the shielding and deshielding effect of the esterified sugar OH towards the esterified secondary alcohol at C–10. When the Mosher reaction is used to assign a stereocentre of a polyfunctional compound, the stereocentre can be considered independent of other stereocentres with secondary alcohols only when they are significantly far apart (Hoye et al. 2007, Seco et al. 2012). During the Mosher analysis, anisotropic effects (shielding/deshielding) of esterified sugar secondary OH groups towards the chiral centre at C–10 were disregarded as it found that these distances were ∼3–4 times that of the distance between C–10 and the chiral carbon of the directly attached MTPA group when monitored during 1 ns *ab-initio* molecular dynamics (AIMD) simulations using the GFN2-xTB extended tight-binding electronic structure approach (Table S3). Thus, the calculation of the stereo configuration at C–10 was carried out independently (Hoye et al. 2007, Seco et al. 2012). The chemical shift difference between the neighbouring protons of the chiral center at C–10 of the (S)-MTPA ester and the (R)–MTPA ester allowed the assignment of the C–10 chiral centre to have an S-configuration (Fig. 4). During the generation of the lowest energy conformers of compound **1** with both (R)- and (S)-MTPA groups at the GFN2-xTB level for use in the AIMD simulations, it was found that the *cis*-form of the amide bond was preferred. As this could have potentially been due to a deficiency of the GFN2-xTB method, this result was checked by comparing the energetics of *cis*- and *trans*-amide conformations of a model of the aromatic core of **1** at the r2SCAN-D4/Def2-QZVP level of theory, which indicated a large preference for the *cis*-form in this structure (Table S4). It is worth noting that the occurrence of *cis* amide bonds is rare in proteins and peptides due to unfavourable constrain between adjacent amino acid residues. Only a handful of naturally occurring peptides with *cis* amide bonds were traced in the literature. The SciFinder search of the core structure of sydosine indicated that only one related compound, phorioadenosine A, was isolated before from an Australian marine sponge *Phoriospongia* sp. (Farrugia et al. 2014).

Compounds **2** and **3** were identified as brefeldin A (**2**; Gorst-Allman et al. 1982, Glaser et al. 2000) phenamide (**3**; Makkar et al. 1995), respectively, by comparing the HRESIMS, NMR, and optical rotation data with the published literature. The following plausible biosynthetic pathway (Fig. 5) is proposed for the new adenosine-nucleoside derivative (**1**). The compound could be derived from the condensation of adenosine (A) and 3-phenyllactic acid (B). Transamination of phenylalanine to phenylpyruvic acid and further reduction take place to synthesize 3-phenyllactic acid (Chaudhari and Gokhale 2016). The biosynthesis of adenosine is well studied, and many comprehensive articles are available (Moffatt and Ashihara 2002). Thus far, natural adenosine-nucleoside derivatives discovered were biosynthesized through the modifications at the exocyclic amine group or the N-containing heteroaromatic ring or the methylene group at the β-ribose sugar unit (Samsel and Dzierbicka 2011, Wang et al. 2018, Valdes et al. 2019, Ariantari et al. 2020, Nguyen et al. 2022). Recent drug discovery efforts to search antibiotics for African Trypanosomiasis (sleeping sickness) caused by the pathogen *Trypanosoma brucei* identified adenosine-nucleosides are the potent drug candidates due to the inhibition of the polyamines biosynthesis, which is critical for the survival of trypanosomes (Hirth et al. 2009, Phillips 2018). Polyamines are multiple amine-substituted aliphatic chains that are essential for the growth of eukaryotes like trypanosomes. Adenosine-nucleosides specifically inhibits the

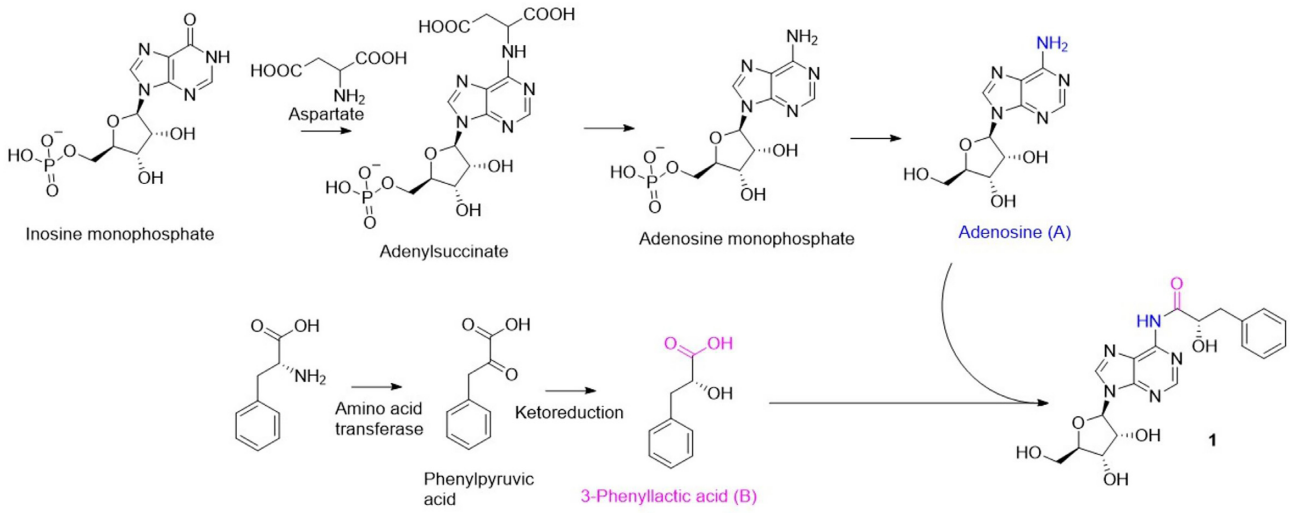

Figure 5. Plausible biosynthetic pathway for the compound **1**.

enzyme S-adenosylmethionine decarboxylase (AdoMetDC), catalysed the biosynthesis of polyamines (Bacchi et al. 1977, Hirth et al. 2009). Thus, we believe, (S)-sydosine could be a great drug candidate for treating anti-protozoan infections, which will be conducted at a future study.

Antimicrobial activity

During the initial antibacterial assessment using Kirby–Bauer disk diffusion assay, only compound **3** showed inhibitory activity against *S. aureus* with a good zone of inhibition (30 mm), and MIC of 0.04 μg/mL, which is two-fold higher than the reference standard rifampicin (MIC = 0.02 μg/mL) (Table S5). Previous studies on compound **3** showed the fungicidal activity against the phytopathogen *Septoria nodorum*, which causes wheat glume blotch. This is the first report on compound **3** from marine *A. sydowii* and its antibacterial activity. Several adenosine-nucleosides have been discovered from natural sources and exhibited diverse *in vitro* biological activities (Wang et al. 2018, Ariantari et al. 2020, Xue et al. 2020). Neither the new adenosine compound **1** nor macrolide brefeldin A (**2**) exhibited antimicrobial activity against the tested bacterial pathogens.

The marine environment is a prolific source for the discovery of fungal diversity. *Aspergillus* species are known to be ubiquitous in their occurrence and the marine *Aspergillus* species are known to produce chemically and biologically diverse metabolites. In this study, a fungal strain MBC15-11F was isolated from the lumen sample of the amphipod *Eurythenes gryllus* that was collected from a previously unexplored location in the North Atlantic Ocean and identified as *Aspergillus sydowii* using ITS, 28S, and β-tubulin sequences. Chemical profiling of the total crude extract of the *A. sydowi* MBC15-11F using LC–HRESIMS analysis showed diverse structural metabolites, including a new hit. In-depth chromatographic and spectroscopic analyses of the fermented fungal broth furnished the new adenosine derivative, which is identified during the dereplication and previously isolated phenylalanine derivative that showed antimicrobial activity for the first time from *Aspergillus*. Due to the scarcity of (S)-sydosine, we proposed the use of combined Mosher analysis and molecular modelling to assign its absolute stereochemistry without sugar hydrolysis. We propose using this approach for absolute configuration determination of sugar-containing metabolites that have distant OH groups in their aglycone. The study confirms that under-explored marine habitats are still a prolific source to discover new marine natural products.

Acknowledgements

Dr Chun Li is acknowledged for the amplification and sequencing of marker genes.

Supplementary data

Supplementary data is available at *JAMBIO Journal* online.

Conflicts of interest

The authors declare no conflict of interest.

Funding

The authors extend their appreciation to the Researchers Supporting Project number (RSP2023R431), King Saud University, Riyadh, Saudi Arabia, for funding this research work. M.Q. would like to thank the support of the EU-Erasmus Mundus-gLINK project (552099-EM-1–2014-1-UK-ERA) for offering the research scholarship to carry out research at the UWS, UK. T.R. would like to thank the Centre for New Antibacterial Strategies (CANS) at UiT the Arctic University of Norway for funding.

Author contributions

Mallique Qader (Formal analysis, Methodology, Software, Validation, Writing – original draft, Writing – review & editing), Larry L. Mweetwa (Formal analysis, Methodology, Resources, Software, Visualization, Writing – original draft), Teppo Rämä (Formal analysis, Methodology, Software, Validation, Writing – review & editing), Bathini Thissera (Formal analysis, Investigation, Methodology, Writing – original draft), Bruce F. Milne (Formal analysis, Methodology,

Software, Visualization), Usama R. Abdelmohsen (Data curation, Formal analysis, Methodology, Software, Writing – original draft), Raha Orfali (Funding acquisition, Investigation, Resources, Software, Visualization, Writing – original draft), Ahmed Tawfike (Formal analysis, Methodology, Software, Writing – original draft), Manal Esheli (Data curation, Software, Validation, Writing – original draft), Emmanuel T. Oluwabusola (Formal analysis, Methodology, Resources, Validation, Writing – original draft), Lalith Jaysainghe (Conceptualization, Data curation, Supervision, Writing – review & editing), Marcel Jaspars (Conceptualization, Investigation, Resources, Supervision, Writing – review & editing) and Mostafa E. Rateb (Conceptualization, Data curation, Formal analysis, Investigation, Methodology, Project administration, Software, Supervision, Validation, Writing – review & editing).

Data availability

The original contributions presented in the study are included in the article/Supplementary Material, further inquiries can be directed to the corresponding author.

References

Abdelmohsen UR, Cheng C, Viegelmann C *et al*. Dereplication strategies for targeted isolation of new antitrypanosomal actinosporins a and B from a marine sponge associated-*Actinokineospora* sp. EG49. *Marine Drugs* 2014;**12**:1220–44. https://doi.org/10.3390/md12031220.

Alvi KA, Nair BG, Rabenstein J *et al*. CD45 tyrosine phosphatase inhibitory components from *Aspergillus niger*. *J Antibiot (Tokyo)* 2000;**53**:110–3. https://doi.org/10.7164/antibiotics.53.110.

Ariantari NP, Ancheeva E, Frank M *et al*. Didymellanosine, a new decahydrofluorene analog, and ascolactone C from *Didymella* sp. IEA-3B. 1, an endophyte of *Terminalia catappa*. *RSC Adv* 2020;**10**:7232–40. https://doi.org/10.1039/C9RA10685E.

Bacchi CJ, Lipschik GY, Nathan HC. Polyamines in trypanosomatids. *J Bacteriol* 1977;**131**:657–61. https://doi.org/10.1128/jb.131.2.657-661.1977.

Bannwarth C, Caldeweyher E, Ehlert S *et al*. Extended tight-binding quantum chemistry methods. *Wiley Interdiscip Rev Comput Mol Sci* 2021;**11**:e1493.

Bannwarth C, Ehlert S, Grimme S. GFN2-xTB—an accurate and broadly parametrized self-consistent tight-binding quantum chemical method with multipole electrostatics and density-dependent dispersion contributions. *J Chem Theory Comput* 2019;**15**:1652–71. https://doi.org/10.1021/acs.jctc.8b01176.

Benson DA, Karsch-Mizrachi I, Lipman DJ *et al*. GenBank. *Nucleic Acids Res* 2005;**33**:D34–8. https://doi.org/10.1093/nar/gki063.

Bhakuni DS, Rawat DS. Bioactive metabolites of marine algae, fungi, and bacteria. *Bioactive Mar Nat Prod* 2005;1–25. https://doi.org/10.1007/1-4020-3484-9_1.

Caldeweyher E, Bannwarth C, Grimme S. Extension of the D3 dispersion coefficient model. *J Chem Phys* 2017;**147**:034112. https://doi.org/10.1063/1.4993215.

Caldeweyher E, Ehlert S, Hansen A *et al*. A generally applicable atomic-charge dependent London dispersion correction. *J Chem Phys* 2019;**150**:154122. https://doi.org/10.1063/1.5090222.

Caldeweyher E, Mewes JM, Ehlert S *et al*. Extension and evaluation of the D4 London-dispersion model for periodic systems. *Phys Chem Chem Phys* 2020;**22**:8499–512. https://doi.org/10.1039/D0CP00502A.

Carroll AR, Copp BR, Davis RA *et al*. Marine natural products. *Nat Prod Rep* 2021;**38**:362–413. https://doi.org/10.1039/D0NP00089B.

Chaudhari SS, Gokhale DV. Phenyllactic acid: a potential antimicrobial compound in lactic acid bacteria. *J Bacteriol Mycol Open Access* 2016; **2**. https://doi.org/10.15406/jbmoa.2016.02.00037.

Ciuffreda P, Casati S, Manzocchi A. Complete 1H and 13C NMR spectral assignment of α-and β-adenosine, 2′-deoxyadenosine, and their acetate derivatives. *Magn Reson Chem* 2007;**45**:781–4. https://doi.org/10.1002/mrc.2036.

Debbab A, Aly AH, Lin WH *et al*. Bioactive compounds from marine bacteria and fungi. *Microb Biotechnol* 2010;**3**:544–63. https://doi.org/10.1111/j.1751-7915.2010.00179.x.

Ehlert S, Huniar U, Ning J *et al*. r2SCAN-D4: dispersion corrected meta-generalized gradient approximation for general chemical applications. *J Chem Phys* 2021;**154**:061101. https://doi.org/10.1063/5.0041008.

Ein-Gil N, Ilan M, Carmeli S *et al*. Presence of *Aspergillus sydowii*, a pathogen of Gorgonian sea fans in the marine sponge *Spongia Obscura*. *ISME J* 2009;**3**:752–5. https://doi.org/10.1038/ismej.2009.18.

Farrugia M, Trotter N, Vijayasarathy S *et al*. Isolation and synthesis of N-acyl adenine and adenosine alkaloids from a southern Australian marine sponge, *Phoriospongia* sp. *Tetrahedron Lett* 2014;**55**:5902–4. https://doi.org/10.1016/j.tetlet.2014.08.116.

Furness JW, Kaplan AD, Ning J *et al*. Accurate and numerically efficient r2SCAN meta-generalized gradient approximation. *J Phys Chem Lett* 2020b;**11**:8208–15. https://doi.org/10.1021/acs.jpclett.0c02405.

Furness JW, Kaplan AD, Ning J *et al*. Correction to accurate and numerically efficient r2SCAN meta-generalized gradient approximation. *J Phys Chem Lett* 2020a;**11**:9248. https://doi.org/10.1021/acs.jpclett.0c03077.

Glaser R, Shiftan D, Froimowitz M. NMR structure determination of brefeldin-A, a 13-membered ring fungal metabolite. *Magn Reson Chem* 2000;**38**:274–80. https://doi.org/10.1002/(SICI)1097-458X(200004)38:4%3c274::AID-MRC630%3e3.0.CO;2-M.

Gorst-Allman CP, Steyn PS, Rabie CJ. 7-epi-brefeldin a, a co-metabolite of brefeldin A in *Curvularia lunata*. *J Chem Soc Perkin Trans* 1982;**1**:2387–90. https://doi.org/10.1039/p19820002387.

Grimme S, Bohle F, Hansen A *et al*. Efficient quantum chemical calculation of structure ensembles and free energies for nonrigid molecules. *J Phys Chem A* 2021;**125**:4039–54. https://doi.org/10.1021/acs.jpca.1c00971.

Hanwell MD, Curtis DE, Lonie DC *et al*. Avogadro: an advanced semantic chemical editor, visualization, and analysis platform. *J Cheminform* 2012;**4**:1–17. https://doi.org/10.1186/1758-2946-4-17.

Hayashi A, Crombie A, Lacey E *et al*. *Aspergillus sydowii* marine fungal bloom in Australian coastal waters, its metabolites, and potential impact on *Symbiodinium dinoflagellates*. *Marine Drugs* 2016;**14**:59. https://doi.org/10.3390/md14030059.

Hirth B, Barker RH, Jr, Celatka CA *et al*. Discovery of new S-adenosylmethionine decarboxylase inhibitors for the treatment of Human African Trypanosomiasis (HAT). *Bioorg Med Chem Lett* 2009;**19**:2916–9. https://doi.org/10.1016/j.bmcl.2009.04.096.

Hoye TR, Jeffrey CS, Shao F. Mosher ester analysis for the determination of the absolute configuration of stereogenic (chiral) carbinol carbons. *Nat Protoc* 2007;**2**:2451–8. https://doi.org/10.1038/nprot.2007.354.

Hudzicki J. Kirby-Bauer disk diffusion susceptibility test protocol. *Am Soc Microbiol* 2009;**15**:55–63. http://www.asmscience.org/content/education/protocol/protocol.3189 (25th September 2021, date last accessed).

Huelsenbeck JP, Ronquist F. MRBAYES: bayesian inference of phylogenetic trees. *Bioinformatics* 2001;**17**:754–5. https://doi.org/10.1093/bioinformatics/17.8.754.

Jalal MAF, Mocharla R, van der Helm D. Separation of ferrichromes and other hydroxamate siderophores of fungal origin by reversed-phase chromatography. *J Chromatogr A* 1984;**301**:247–52. https://doi.org/10.1016/S0021-9673(01)89192-5.

Katoh K, Misawa K, Kuma KI *et al*. MAFFT: a Novel method for rapid multiple sequence alignments based on fast fourier transform. *Nu-*

cleic Acids Res 2002;**30**:3059–66. https://doi.org/10.1093/nar/gkf436.

Katoh K, Standley DM. MAFFT multiple sequence alignment software version 7: improvements in performance and usability. *Mol Biol Evol* 2013;**30**:772–80. https://doi.org/10.1093/molbev/mst010.

Kildgaard S, Mansson M, Dosen I *et al*. Accurate dereplication of bioactive secondary metabolites from marine-derived fungi by UHPLC-DAD-QTOFMS and an MS/HRMS library. *Marine Drugs* 2014;**12**:3681–705. https://doi.org/10.3390/md12063681.

Lefort V, Longueville JE, Gascuel O. SMS: smart Model selection in PhyML. *Mol Biol Evol* 2017;**34**:2422–4. https://doi.org/10.1093/molbev/msx149.

Li WT, Luo D, Huang JN *et al*. Antibacterial constituents from antarctic fungus, *Aspergillus sydowii* SP-1. *Nat Prod Res* 2018;**32**:662–7. https://doi.org/10.1080/14786419.2017.1335730.

Liang X, Huang ZH, Ma X *et al*. Mycotoxins as inhibitors of protein tyrosine phosphatases from the deep-sea-derived fungus *Aspergillus puniceus* SCSIO z021. *Bioorg Chem* 2021;**107**:104571. https://doi.org/10.1016/j.bioorg.2020.104571.

Lorenz P, Jensen PR, Fenical W. Mactanamide, a new fungistatic diketopiperazine produced by a marine *Aspergillus* sp. *Nat Prod Lett* 1998;**12**:55–60. https://doi.org/10.1080/10575639808048871.

Lotfy MM, Sayed AM, AboulMagd AM *et al*. Metabolomic profiling, biological evaluation of *Aspergillus awamori* , the river Nile-derived fungus using epigenetic and OSMAC approaches. *RSC Adv* 2021;**11**:6709–19. https://doi.org/10.1039/D0RA07578G.

Makkar NS, Nickson TE, Tran M *et al*. Phenamide, a fungicidal metabolite from *Streptomyces albospinus* A19301 taxonomy, fermentation, isolation, physicochemical and biological properties. *J Antibiot (Tokyo)* 1995;**48**:369–74. https://doi.org/10.7164/antibiotics.48.369.

Mennucci B. Polarizable continuum model. *WIREs Comp Mol Sci* 2012;**2**:386–404. https://doi.org/10.1002/wcms.1086.

Moffatt BA, Ashihara H. Purine and pyrimidine nucleotide synthesis and metabolism. *Arabidopsis Book* 2002;**1**. https://doi.org/10.1199/tab.0018.

Murray MG, Thompson W. Rapid isolation of high molecular weight plant DNA. *Nucleic Acids Res* 1980;**8**:4321–6. https://doi.org/10.1093/nar/8.19.4321.

Neese F. Software update: the ORCA program system, version 4.0. *Wiley Interdiscip Rev Comput Mol Sci* 2017;**8**:e1327.

Neese F. The ORCA program system. *Wiley Interdiscip Rev Comput Mol Sci* 2012;**2**:73–78.

Nguyen M, An S, Nguyen Y *et al*. Design, synthesis, and biological activity of l-1′-homologated adenosine derivatives. *ACS Med Chem Lett* 2022;**13**:1131–6. https://doi.org/10.1021/acsmedchemlett.2c00159.

Niu S, Yang L, Chen T *et al*. New monoterpenoids and polyketides from the deep-sea sediment-derived fungus *Aspergillus sydowii* MCCC 3A00324. *Marine Drugs* 2020;**18**:561. https://doi.org/10.3390/md18110561.

Ohtani I, Kusumi T, Kashman Y *et al*. High-field FT NMR application of Mosher's method. The absolute configurations of marine terpenoids. *J Am Chem Soc* 1991;**113**:4092–6. https://doi.org/10.1021/ja00011a006.

Orfali R, Aboseada MA, Abdel-Wahab NM *et al*. Recent updates on the bioactive compounds of the marine-derived genus *Aspergillus*. *RSC Adv* 2021;**11**:17116–50. https://doi.org/10.1039/D1RA01359A.

Pettersen EF, Goddard TD, Huang CC *et al*. UCSF Chimera—a visualization system for exploratory research and analysis. *J Comput Chem* 2004;**25**:1605–12. https://doi.org/10.1002/jcc.20084.

Phillips MA. Polyamines in protozoan pathogens. *J Biol Chem* 2018;**293**:18746–56. https://doi.org/10.1074/jbc.TM118.003342.

Pracht P, Bohle F, Grimme S. Automated exploration of the low-energy chemical space with fast quantum chemical methods. *Phys Chem Chem Phys* 2020;**22**:7169–92. https://doi.org/10.1039/C9CP06869D.

Rämä T, Hassett BT, Bubnova E. Arctic marine fungi: from filaments and flagella to operational taxonomic units and beyond. *Bot Mar* 2017;**60**:433–452. https://doi.org/10.1515/bot-2016-0104.

Ramírez-Camejo LA, Zuluaga-Montero A, Lázaro-Escudero M *et al*. Phylogeography of the cosmopolitan fungus *Aspergillus flavus*: is everything everywhere? *Fungal Biol* 2012;**116**:452–63. https://doi.org/10.1016/j.funbio.2012.01.006.

Rypien KL, Andras JP, Harvell CD. Globally panmictic population structure in the opportunistic fungal pathogen *Aspergillus sydowii*. *Mol Ecol* 2008;**17**:4068–78. https://doi.org/10.1111/j.1365-294X.2008.03894.x.

Samsel M, Dzierzbicka K. Therapeutic potential of adenosine analogues and conjugates. *Pharmacol Rep* 2011;**63**:601–17. https://doi.org/10.1016/S1734-1140(11)70573-4.

Sayed AM, Hassan MH, Alhadrami HA *et al*. Extreme environments: microbiology leading to specialized metabolites. *J Appl Microbiol* 2020;**128**:630–57. https://doi.org/10.1111/jam.14386.

Seco JM, Quiñoá E, Riguera R. Assignment of the absolute configuration of polyfunctional compounds by NMR using chiral derivatizing agents. *Chem Rev* 2012;**112**:4603–41. https://doi.org/10.1021/cr2003344.

Siqueira JPZ, Sutton DA, García D *et al*. Species diversity of *Aspergillus* section *versicolores* in clinical samples and antifungal susceptibility. *Fungal Biology* 2016;**120**:1458–67. https://doi.org/10.1016/j.funbio.2016.02.006.

Stamatakis A. RAxML version 8: a tool for phylogenetic analysis and post-analysis of large phylogenies. *Bioinformatics* 2014;**30**:1312–3. https://doi.org/10.1093/bioinformatics/btu033.

Stamatakis A. RAxML-VI-HPC: maximum likelihood-based phylogenetic analyses with thousands of taxa and mixed models. *Bioinformatics* 2006;**22**:2688–90. https://doi.org/10.1093/bioinformatics/btl446.

Steyn PS, Vleggaar R. Austocystins. Six novel dihydrofuro [3′, 2′: 4, 5] from [3, 2-b] xanthenones from *Aspergillus ustus*. *J Chem Soc Perkin Trans* 1974;**1**:2250–6. https://doi.org/10.1039/P19740002250.

Su BN, Park EJ, Mbwambo ZH *et al*. New chemical constituents of *Euphorbia quinquecostata* and absolute configuration assignment by a convenient Mosher ester procedure carried out in NMR tubes. *J Nat Prod* 2002;**65**:1278–82. https://doi.org/10.1021/np0202475.

Suzuki K, Kuwahara A, Yoshida H *et al*. NF00659A1, A2, A3, B1, and B2: novel antitumor antibiotics produced by *Aspergillus* sp. NF 00659 I. taxonomy, fermentation, isolation, and biological activities. *J Antibiot (Tokyo)* 1997;**50**:314–7. https://doi.org/10.7164/antibiotics.50.314.

Tawfike AF, Viegelmann C, Edrada-Ebel R. Metabolomics and dereplication strategies in natural products. In: Roessner U, Dias D (ed.), *Metabolomics Tools for Natural Product Discovery*. Totowa, NJ. Humana Press, 2013, 227–44. https://doi.org/10.1007/978-1-62703-577-4_17

Tomasi J, Mennucci B, Cammi R. Quantum Mechanical Continuum Solvation Models. *Chem Rev* 2005;**105**:2999–3094. https://doi.org/10.1021/cr9904009.

Tsai HF, Fujii I, Watanabe A *et al*. Pentaketide melanin biosynthesis in *Aspergillus fumigatus* requires chain-length shortening of a heptaketide precursor. *J Biol Chem* 2001;**276**:29292–8. https://doi.org/10.1074/jbc.M101998200.

Valdes F, Brown N, Morales-Bayuelo A *et al*. Adenosine derivates as antioxidant agents: synthesis, characterization, in vitro activity, and theoretical insights. *Antioxidants* 2019;**8**:468. https://doi.org/10.3390/antiox8100468.

Voser TM, Campbell MD, Carroll AR. How different are marine microbial natural products compared to their terrestrial counterparts? *Nat Prod Rep* 2022;**39**. https://doi.org/10.1039/D1NP00051A

Wang ZW, Li Y, Liu DH *et al*. Chemical constituents from the rhizomes of *gastrodia elata* f. *glauca* and their potential neuroprotective effects. *Phytochem Lett* 2018;**24**:167–71. https://doi.org/10.1016/j.phytol.2018.02.010.

Weigend F, Ahlrichs R. Balanced basis sets of split valence, triple zeta valence, and quadruple zeta valence quality for H to Rn: design and assessment of accuracy. *Phys Chem Chem Phys* 2005;**7**:3297–305. https://doi.org/10.1039/b508541a.

Weigend F. Accurate coulomb-fitting basis sets for H to Rn. *Phys Chem Chem Phys* 2006;**8**:1057–65. https://doi.org/10.1039/b515623h.

Xue Y, Wu L, Ding Y *et al*. A new nucleoside and two new pyrrole alkaloid derivatives from *Cordyceps militaris*. *Nat Prod Res* 2020;**34**:341–50. https://doi.org/10.1080/14786419.2018.1531861.

Zain ul Arifeen M, Ma YN, Xue YR *et al*. Deep-sea fungi could be the new arsenal for bioactive molecules. *Marine Drugs* 2019;**18**:9. https://doi.org/10.3390/md18010009.

Zhou Y, Debbab A, Mándi A *et al*. Alkaloids from the sponge-associated fungus *Aspergillus* sp. *Eur J Org Chem* 2013;**2013**:894–906. https://doi.org/10.1002/ejoc.201201220.

Zuck KM, Shipley S, Newman DJ. Induced production of N-formyl alkaloids from *Aspergillus fumigatus* by co-culture with *Streptomyces peucetius*. *J Nat Prod* 2011;**74**:1653–7. https://doi.org/10.1021/np200255f.